The Outphasing RF Power Amplifier: A Comprehensive Analysis and a Class-B CMOS Realization

Shervin Moloudi, *Member, IEEE*, and Asad A. Abidi, *Fellow, IEEE*

***Abstract*—We present a theoretically comprehensive treatment of outphasing systems that utilize radio-frequency high-efficiency PAs. We separately analyze encoding and clipping distortions and how they accounts for most of the nonlinearities in outphasing systems. With that insight, we have designed an inherently linear outphasing system at high efficiency. We have implemented these techniques in a 90-nm Class-B prototype that uses signal-dependent time-varying circuits under close digital control to achieve 56%, 44%, and 30% efficiency for GSM, EDGE, and WCDMA modulations, while demonstrating linearity commensurate with demanding specifications on adjacent channel leakage.**

***Index Terms*—Chireix combiner, Class B, CMOS, efficiency, LINC, linearization, outphasing, power amplifier (PA), power combiner, transmitter.**

I. Background and Introduction

THE power amplifier (PA) modulates, as efficiently as possible, energy it takes from a power supply and delivers it into the load. The widely-used Class B PA [1, Ch. 2] produces an output drain current that is half-wave rectified and distorted by FET input–output nonlinearity. Since distortion leads to half cycles whose shape changes with the amplitude of the input sinewave voltage, there is a nonlinear relation between the amplitude of the fundamental frequency in the spectrum of the output current and the amplitude of the input sinewave. Therefore, to demonstrate an acceptably linear input–output characteristic, the PA must operate well away from compression,[1] where it can translate input amplitude faithfully into the output. This is also where the efficiency falls off; all Class-B PAs in widespread use in mobile RF transmitters pay this penalty. On the other hand, the Class-B PA is able to operate well into compression at its peak efficiency when it carries a waveform modulated only in phase, whose envelope is constant. This arrangement was used in mobile GSM transmitters. However, as constant envelope GSM is retired from service to be replaced with variable envelope modulations, the simple saturated PA operating at constant supply voltage will also fade away.

New methods are being sought to encode arbitrary amplitude and phase modulations on a carrier wave into *purely* phase-modulated waveforms. This, precisely, is the basis for outphasing, a *method for encoding with pure phase modulation*. While the idea behind outphasing is easily understood, conceptual difficulties arise in circuit realization of an *efficient outphasing amplifier*. Identifying these difficulties, analyzing the associated forms of distortion and resolving them is the main thrust of this paper, which will conclude with the experimental demonstration of a correctly formulated outphasing amplifier circuit.

Manuscript received May 07, 2012; revised January 31, 2013; accepted February 25, 2013. Date of publication April 02, 2013; date of current version May 22, 2013. This paper was approved by Associate Editor Jan Cranickx.

S. Moloudi is with Qualcomm-Atheros Inc., Irvine, CA 92618 USA (e-mail: shervin@ucla.edu).

A. A. Abidi is with the University of California, Los Angeles, CA 90095 USA (e-mail: abidi@ee.ucla.edu).

Color versions of one or more of the figures in this paper are available online at http://ieeexplore.ieee.org.

Digital Object Identifier 10.1109/JSSC.2013.2252522

[1]Compression corresponds to the operation mode where an FET goes into triode or a BJT goes into saturation. While saturation is an accepted term to describe PA compression, we do not use it in this paper to avoid confusion with the FET active region, also called saturation.

II. Outphasing Modulation

The waveform $x(t)$ of a carrier wave at radian frequency ω_0 with arbitrary amplitude and phase modulation can always be expressed as [2], [3]

$$x(t) = \mathrm{Re}\left(\gamma(t)\exp(j\omega_0 t)\right) \tag{1}$$

where $\gamma(t)$ is a complex phasor waveform that captures the baseband modulation. If this modulation is taken from a finite codebook of symbols, then the instantaneous magnitude of $x(t)$ has a well-defined maximum X_m, i.e. $0 \leq |x(t)| \leq X_m$. In polar coordinates, the instantaneous magnitude of γ may be expressed as a fraction of X_m, encoded by the $\sin$ of an angle ϕ as

$$\gamma(t) = |\gamma(t)|\exp(j\angle\gamma) = X_m \sin\phi(t)\exp(j\angle\gamma). \tag{2}$$

ϕ is called the *outphasing angle* and belongs to $[0, \pi/2]$. Substituting (2) into (1), we see how outphasing modulation reconstructs $x(t)$ from the difference between *two* constant envelope phase-modulated waveforms (Fig. 1):[2]

$$\begin{aligned} x(t) &= \mathrm{Re}\left(X_m \sin\phi(t)\exp\left(j(\omega_0 t + \angle\gamma)\right)\right) && (3)\\ &= X_m \sin\left(\omega_0 t + \angle\gamma(t) + \phi(t)\right) \\ &\quad - X_m \sin\left(\omega_0 t + \angle\gamma(t) - \phi(t)\right). && (4) \end{aligned}$$

III. Power Combining

The case for the outphasing principle rests on a PA's ability to operate at the peak efficiency when it carries a constant envelope

[2]Another common but slightly different arrangement reconstructs $x(t)$ from the sum of two constant envelope waveforms.

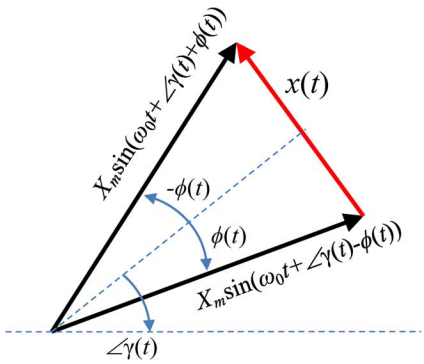

Fig. 1. Arbitrary modulation and its outphasing components.

but phase-modulated waveform. In theory, therefore, arbitrary modulations encoded by two such waveforms can be amplified by two PAs, each PA operating at its maximum efficiency. $x(t)$ is reconstructed in the eventual load according to (4) by summing the amplified output powers from the two PAs into the load without reflections in a three-port attached to the PAs and the load. Therefore, we need a lossless, reciprocal (for practical realization at RF) three-port, which is matched at two of its ports to the impedance of an antenna that attaches to the third port.

A three-port with these features is physically unrealizable [4, p. 277], [5, p. 309] since a lossless three-port *must* always reflect some of the power incident on any one port and distribute portions of the power entering that port to the other two ports. This is why the ports cannot all be impedance-matched simultaneously, except for the trivial case when two ports are driven by identical voltages. At the heart of these considerations is the principle of conservation of energy: if the power into two ports driven by outphased sinewaves combines without loss into a load attached to the third port, then, as the outphasing angle approaches zero, the "destructive interference" at the third port means that no energy is delivered to the load. This implies that each source must perceive a nonabsorbing impedance across its terminals, which can only be a pure reactance. Therefore, the port impedance changes from a resistance at large ϕ to a reactance at small ϕ. Impedance matching does not hold across phase.

However, simultaneous matching of ports is possible in a four-port, with sources connected at two of the ports and equal load resistances at the other two ports. When the two sources generate in-phase sinewaves of equal amplitude, they may add at one of the load resistors to deliver a maximum of power, but subtract at the other load resistor, which will act as a dummy. If they are anti-phase, the situation at the two load resistors will reverse. For intermediate phase differences between these two extremes, nonzero voltages will appear across both load resistors and apportion power between them. Now, energy conservation can no longer rule out that the driving point resistance at the ports remains constant under all cases.

Previous outphasing amplifiers have used a four-port lossy power combiner as described above [4, p. 281], [5, p. 313] and, in doing so, have sacrificed power conversion efficiency by up to 50% because of dissipation in the dummy load. It has been proposed [6] that the power dissipated in the dummy resistor may be recovered and recycled, and improvements in efficiency and linearity of this scheme has been recently demonstrated [7].

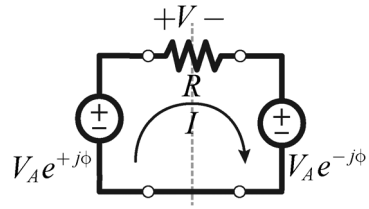

Fig. 2. Ideal outphasing circuit.

However, the reported performance depends significantly on the choice of rectifier used in the energy recycling module and it is hard to find rectifiers that perform well under high-power *and* high-frequency conditions. These rectifiers and the considerable number of passive components involved limit the use of this approach in an integrated context. Alternatively, we can pursue combining power in a lossless three-port and find a remedy for the changing impedances. While in the original outphasing paper Chireix [8] himself explores this line of thinking at some length, the literature on outphasing amplifiers since then has not sufficiently addressed the problems of lossless power combining in practical implementations.

A. Outphasing as a Circuits Concept

Consider the two terminals of a resistor R (Fig. 2) driven at some frequency by two sinusoidal *voltage sources* of equal amplitude[3] expressed, respectively, by phasors $V_A e^{+j\phi}$ and $V_A e^{-j\phi}$. The voltage across the resistor is equal to $2jV_A \sin\phi$. Therefore, as the phase angle ϕ changes, it regulates the load voltage and thereby the power that dissipates in R from constant amplitude voltage sources. This is outphasing as defined in (4) reduced to the simplest possible circuit.

Let us rediagram Fig. 2 as a three-port (Fig. 3), where $V_A e^{+j\phi}$ is an independent voltage source that controls[4] the voltage source $V_A e^{-j\phi}$. The driving point admittance across the terminals of the independent source $V_A e^{+j\phi}$ can be derived as

$$Y_1(\phi) \stackrel{\text{def}}{=} G(\phi) + jB(\phi) = \frac{2\sin^2\phi}{R} + j\frac{\sin 2\phi}{R}. \tag{5}$$

By reversing the argument, it follows that the admittance across the terminals of the source $V_A e^{-j\phi}$ is

$$\begin{aligned} Y_2(\phi) &= Y_1(-\phi) \\ &= G(\phi) - jB(\phi) \\ &= \frac{2\sin^2\phi}{R} - j\frac{\sin 2\phi}{R}. \end{aligned} \tag{6}$$

As ϕ changes, the real part of the admittance across each source also changes to extract equal amounts of real power from each source, amounting to a total real power dissipated in the load R of

$$P_{\text{Re}}(\phi) = 2 \times \frac{1}{2} V_A^2 G(\phi) = 2\frac{V_A^2}{R}\sin^2\phi. \tag{7}$$

[3][9] and [10, Fig. 2.21] were among the first to describe outphasing in this essential format, shorn of unnecessary appendages.

[4]This is best understood by composing $V_A e^{+j\phi}$ as two phasor sources in series $V_A \cos\phi$ and $jV_A \sin\phi$, which control two other *dependent* sources with gains $+1$ and -1, respectively.

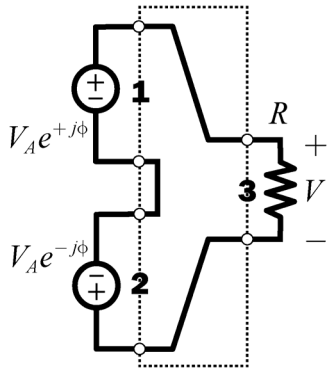

Fig. 3. Ideal outphasing circuit, redrawn as a three-port.

However, this equivalent circuit also reveals that there is a flow of imaginary, or reactive power [11], *out of* one source and *into* the other. This is a circulating power of magnitude

$$P_{\mathrm{Im}}(\phi) = \frac{1}{2}V_A^2 B(\phi) = \frac{V_A^2}{R}\sin\phi\cdot\cos\phi. \tag{8}$$

It is customary to measure real power as a fraction of the total complex power by the power factor (PF). The closer the PF is to 1, the more the driving point admittance appears as a pure resistor. Expressed in terms of driving point admittance [11] $G + jB$, we have

$$\begin{aligned} PF &= \cos\left(\arctan\left(\frac{B}{G}\right)\right) \\ &= \cos\left(\arctan(\cot\phi)\right) \\ &= \cos(90^\circ - \phi) = \sin\phi. \end{aligned} \tag{9}$$

When $\phi \simeq 0$, we see in the simple circuit of Fig. 2 that both ends of the load R are driven by almost the same voltage, so it dissipates nearly zero power. When the same circuit is viewed as a three port, each source is driving a load with $PF \simeq 0$, that is, a load that appears almost purely imaginary with a very small susceptance. As $\phi \to 90^\circ$, the $PF \to 1$ which means that the load across each voltage source appears almost purely resistive, as it should be. For outphasing angles in the middle, each source perceives a load that is mixed resistive and reactive, specified by the PF. By regulating the PF of the "apparent load" across each of two voltage sources with equal and constant amplitude, the outphasing angle ϕ changes the real power that flows from them or *outphasing modulates the load voltage by changing the power factor across the terminals of two voltage sources energizing the load*.

B. Power Factor Correction and Some Consequences

A lossless load like a capacitor or inductor will absorb an average of zero power from a sinusoidal voltage or current. However, if this sinewave is supplied by an amplifier, the amplifier's transistors will dissipate some real power even when the load does not. For example, each of the complementary pair of transistors in a push-pull Class B amplifier supplies a half cycle of sinewave current to a resistor load. This is also true when the resistor is replaced by a capacitor C. If the two supplies are labeled $\pm V_{\mathrm{DD}}$ and the load voltage is $V_P\cos(2\pi ft)$, each transistor will draw an average current from its supply of $2fCV_P$, and together the two transistors will dissipate a power $4fCV_PV_{\mathrm{DD}}$. This result can be checked readily.[5]

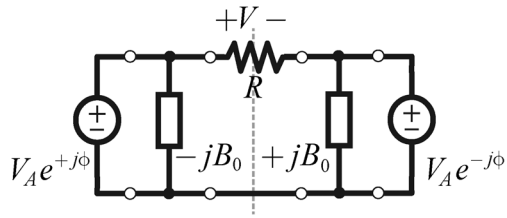

Fig. 4. Chireix compensation to improve average power factor.

This has clear repercussions for an outphasing PA. When, during outphasing, the PF of the apparent load falls substantially below 1, the transistors that realize the voltage sources may dissipate increasing amounts of real power to service the growing reactive portion of load current. This is bad for efficiency. Chireix [8] proposed as a remedy the use of PF correction, an idea well known at the time in connection with ac power distribution. Over the range $\phi : 0 \to 90^\circ$ the apparent susceptance across one voltage source will appear increasingly positive (that is, relatively more capacitive) while across the other voltage source it will appear increasingly negative (that is, relatively inductive). The ideal solution is to insert a tracking inductance across the first source and a tracking capacitance across the other source to cancel the apparent reactances at the carrier frequency of operation. But it is not easy to realize continuously variable reactances, at least in Chireix's time. Instead, he showed that on the balance there would be an improvement in efficiency if by inserting fixed susceptances the PF was exactly corrected at only one outphasing angle (Fig. 4). If the correction is realized close to $\phi = 90^\circ$ when the load current is highest, then, far away towards 0°, the PF will be off, but since the load currents are small, the error will not matter as much. As an example, he showed that exact correction at $\phi = 72^\circ$[6] keeps $PF > 0.88$ across much of the remaining range of outphasing angles. This method of improving an outphasing amplifier's PF, and, thus, its efficiency goes by the name of *Chireix compensation*.

While Chireix compensation makes the apparent load across each voltage source look resistive over most of the angular range, that resistance is not constant but changes with output amplitude, following the real part of (5) and (6). This means that, if the voltage sources are replaced with PA circuits, those circuits must operate with changing load. Simple Class-A and Class-B amplifiers can handle variable load resistance up to a certain limit without waveform distortion but with changing efficiency. Eventually, an extreme load resistance will push them into compression with untoward consequences on distortion, as we will discuss later in Section III-C.

Class-D amplifiers are the closest to ideal voltage sources. Successful implementations of outphasing amplifiers with Class-D PAs have been reported, most notably in [12]. Class-D

[5]When $V_P = V_{\mathrm{DD}}$, this power becomes $4fCV_{\mathrm{DD}}^2$. This is the classic expression for the power dissipated by the FETs in a CMOS inverter as they switch a load C at frequency f between $\pm V_{\mathrm{DD}}$. The power dissipated is actually equal, whether the capacitor is switched by a square wave, or, as in our case, driven by a Class-B PA to a sinewave voltage of $2V_{\mathrm{DD}}$ peak-to-peak.

[6]His paper shows $\phi = 18^\circ = \pi/10$ rad because he used the convention of adding outphasing vectors to construct $x(t)$.

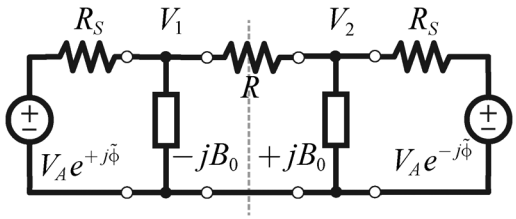

Fig. 5. Chireix compensation, including source resistance.

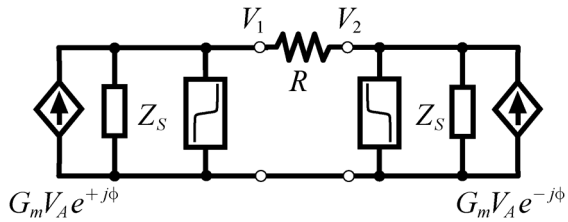

Fig. 6. Equivalent circuit with Class-B PAs modeled as current sources, with voltage limiting nonlinear shunt elements.

amplifiers in a given technology will always be limited to operation at frequencies well below f_T, otherwise losses arising from capacitive currents that worsen with frequency will significantly erode efficiency. Even if the loss in efficiency were tolerable, as the switching time of the amplifier FETs approaches a few percent of the period of the carrier, the modulated spectrum shows distortion. This is explained in [12].

More sophisticated arrangements like Class E and F achieve high efficiency through careful waveshaping. In Class-E PAs, the average dissipation is minimized through a lossless single-terminated LC two-port that absorbs the transistor capacitance [13]. However, when the apparent load changes substantially with outphasing angle, the optimum wave shaping is lost. Therefore, it is difficult to see how a Class-E amplifier that uses a fixed, time-invariant waveshaping network can yield its full efficiency in an outphasing architecture with lossless combining [14]. The resonance tank in a Class-F amplifier has a driving point impedance with nulls and singularities at harmonics [15]. While the number of passive components needed to accomplish this can make discrete implementations expensive and integrated realizations suboptimal (due to the lossy nature of integrated passive elements) it can still be a candidate for an outphasing PA. An extensive analysis can be found in [14].

In [16], Birafane and Kouki report an unexpected outcome of Chireix compensation. They have simulated a realistic equivalent circuit of a Chireix-compensated outphasing amplifier, represented by a simple circuit in which a non-zero source resistance R_S is added in series with each voltage source (Fig. 5). Chireix compensation in the form of two susceptances $\pm B_0$ is introduced. Clearly, as $B_0 \to 0$, the compensation disappears. The reported simulations show that with stronger compensation (larger B_0), an increasing *nonlinearity* appears in the amplifier output, leading to the incorrect suggestion that the outphasing amplifier trades off efficiency against linearity.

To properly explain this nonlinearity, we note that the Chireix compensation susceptances destroy the bilateral symmetry of the circuit, so the drive across the load resistor R no longer resolves into a simple expression in $\sin\phi$. Instead, the load voltage is now governed by a modified outphasing relation

$$(V_1 - V_2) = V_A \frac{2j\sqrt{1 + B_0^2 R_S^2}}{2\frac{R_S}{R} + B_0^2 R_S^2 + 1} \sin(\phi + \alpha) \qquad (10)$$

where $\alpha = \arctan(B_0 R_S)$. This has been also noted in [17]. If, unaware of the offset in the argument of the nonlinear $\sin$ function one continues to encode the output amplitude as $V_A \sin\phi$, a distortion must appear associated simply with the nonlinearity of a trigonometric function. On the other hand when the amplitude is correctly encoded as $V_A \sin(\phi + \alpha)$ the distortion will disappear. This *encoding distortion* may be removed by a simple rotation of the outphasing angle, and a scaling of the output amplitude.

C. PA Compression

Even the fastest CMOS FETs available today cannot implement, at, say, 6 GHz, a true switching amplifier that operates in Class D mode. The FET would have to transition from the OFF state to deep triode in a fraction of the RF cycle. It is more likely that over most of the cycle the load and parasitic reactances will force the FET to traverse different regions of its $I-V$ characteristic as it continues to operate away from the triode region. Over this transition it is more accurately modeled by a large-signal voltage-controlled *current source* [13, Sec. II-A]. If, in the absence of a signal the FET is biased close to threshold for high efficiency, then a large RF input signal will force it into Class-B operation. In other words, when true Class-D operation fails at very high switching frequencies, the transistor reverts to Class B.

To model this Class-B PA we use a linear large-signal transconductor G_m (Fig. 6) with some output impedance Z_S that is generally much larger than the load R. As the instantaneous voltage across the ideal current source approaches either 0 or the supply $V_{\rm DD}$, the nonlinear voltage limiter connected across the terminals will model clipping. G_m and Z_S have now replaced the *voltage sources* of Fig. 2. However, replacing a voltage source with a current source without also changing the topology of the circuit into its dual [11] creates a fundamentally different circuit with unforeseen aspects to its behavior.

If the voltage inputs to the transconductors are $V_A e^{\pm j\phi}$, straightforward derivations yield

$$V_{1,2} = G_m Z_S V_A \cos\phi \pm jG_m(Z_S \| R/2) V_A \sin\phi \qquad (11)$$

$$\simeq G_m Z_S V_A \cos\phi \pm jG_m \left(\frac{R}{2}\right) V_A \sin\phi. \qquad (12)$$

At $\phi = 90°$, the PAs drive the combiner differentially and each one sees a fixed resistance of $R/2$. For the sake of efficiency, the amplifiers are designed to operate at or near compression for this value of ϕ. As ϕ decreases, the PA output swings will increase according to (11) because $Z_S \gg R$ means that the real part is much larger than the imaginary part. Although V_1 and V_2 do not remain at constant amplitude, the load voltage still follows the outphasing form:

$$V_1 - V_2 = 2jG_m(Z_S \| R/2) V_A \sin\phi$$

$$\simeq jG_m R V_A \sin\phi. \qquad (13)$$

The implication is that, although Class-B amplifiers do not act as ideal voltage sources, they can still generate the right

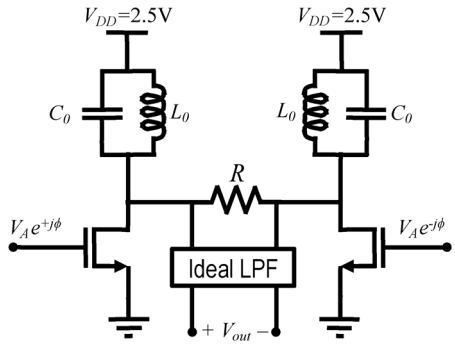

Fig. 7. Clipping distortion simulation setup.

waveform across the load if their transconductances remain constant. However, this is only the case when the Class B is not pushed into compression, at which point the transconductance collapses. As ϕ goes from 90° to zero, the magnitude of the voltage swing across each Class-B PA changes from $G_m(R/2)V_A$ to $G_m Z_S V_A$, which will almost certainly compress the amplifier. In other words, so that the load carries zero current at low ϕ, the current sources must force all of their current into their own output resistances. Since a good current source's output resistance is large, the voltage swing across each source will rise to the point that it pushes the FETs making up that current source into compression. Therefore G_m in (13) will vary, the outphasing relationship at the load will break, and distortion will appear. Unlike the encoding distortion which can be fixed by a linear transformation, the *clipping distortion* cannot be corrected.

We simulated an outphasing PA comprising two FETs operating in Class B with their outputs coupled directly to a load (Fig. 7). An ideal low-pass filter at the output removes the harmonics of the carrier. Distortion is seen (Fig. 8) when the simulated load voltage is compared with the ideal modulation. The output of one core PA is also plotted in this figure. Since each PA is connected to a supply of 2.5 V through an inductively tuned load, the output voltage will swing form above 0 to slightly below 5 V while the FET is in active region. A closer inspection of this waveform shows that the swing varies with the outphasing angle as predicted by (11). At point A, where the output is at its peak, i.e., ϕ is close to 90°, the core PA swings to just below 5 V. When ϕ decreases, the core PA is pushed into deep triode and the swing pushes up to about 5.7 V (point B). Now, G_m drops and distortion becomes visible.

It is therefore expected that, when lossless combining is used without Chireix compensation, clipping distortion will almost certainly appear. [18] presents a simulated output spectrum of a CDMA waveform after lossless combining in a Class-E outphasing PA, where the simulated spectral density in adjacent channels is down by only −50 dB, when it should theoretically be lower than −80 dB. FETs in an outphasing arrangement with lossless combining cannot remain in Class E operation when they face a changing apparent load; therefore, it is likely that encoding and clipping distortions described above are at work in this circuit and account for the nonideal spectrum. [19] reports on an experimental CMOS realization of this Class-E PA at 8 GHz with measured spectrum almost identical to what was simulated in [18].

Chireix compensation will not make clipping distortion go away. With the compensating susceptances, (11) is modified to

$$V_{1,2} = G_m Z_S V_A \frac{R+2Z_S}{R(1+Z_S^2B_0^2)+2Z_S}\cos\phi \pm jG_m Z_S V_A \frac{R\sqrt{1+Z_S^2B_0^2}}{R(1+Z_S^2B_0^2)+2Z_S}\sin(\phi+\alpha) \quad (14)$$

with α defined in (10). The problem again arises from the real term, which despite the mitigating factor $((R+2Z_S)/(R(1+Z_S^2B_0^2)+2Z_S)) < 1$ can still become sufficiently large for small ϕ to push the PAs into deep compression. This is also confirmed by our simulations.

In [17], the authors, aware of encoding distortion, compensate for α in their Class B outphasing amplifier. Nonetheless, with lossless combining they continue to observe an unexplained residual distortion, which disappears when a lossy Wilkinson power combiner [5, p. 318] is used. Since a lossy combiner isolates the two Class-B amplifiers, we now show that the remaining distortion is due to clipping in the Class-B PAs.

The exact nature of the compression in a PA depends largely on the inherent nonlinearities of the underlying devices. To emulate the pHEMT amplifier used in [17], we turn to Rapp's model [20], which has been widely used to capture the gradual compression in high-power microwave PAs. It describes a saturating voltage $\tilde{V}_1$ at the output of the controlled sources in Fig. 6 with the expression

$$\tilde{V}_1 = \frac{V_1}{\sqrt{1+\left(\frac{V_1}{V_{sat}}\right)^2}} \quad (15)$$

where V_1 would be the voltage with no clipping. A simple numerical simulation of the voltage across the terminals of each transistor can reproduce a nonlinear characteristic (Fig. 9) that closely matches the reported measurements in [17, Fig. 16].

D. Spectral Leakage From Path Mismatch

Outphasing is vulnerable to errors arising from mismatch between the signal paths. Suppose the amplitude of one outphasing voltage is $(1+\epsilon)$ times as large as the other, and that the outphasing drive to it is delayed by a constant phase δ over a narrow band around the carrier frequency ω_0. Then, the reconstructed waveform $\tilde{x}(t)$ is given by

$$\begin{aligned}\tilde{x}(t) &= \mathrm{Re}\left[X_m\left((1+\epsilon)\exp j\left(\omega_0 t+\angle\gamma(t)+\phi(t)+\delta\right)\right.\right.\\ &\qquad \left.\left.+\exp j\left(\omega_0 t+\angle\gamma(t)-\phi(t)\right)\right)\right]\\ &\simeq \mathrm{Re}\left[X_m\left(\exp j\left(\omega_0 t+\angle\gamma(t)+\phi(t)\right)\right.\right.\\ &\qquad \left.+\exp j\left(\omega_0 t+\angle\gamma(t)-\phi(t)\right)\right)\\ &\qquad \left.+X_m(\epsilon+j\delta)\exp j\left(\omega_0 t+\angle\gamma(t)+\phi(t)\right)\right].\end{aligned}$$

Therefore

$$\tilde{x}(t) = x(t) + X_m\left(\epsilon\cos\left(\omega_0 t+\angle\gamma(t)+\phi(t)\right) - \delta\sin\left(\omega_0 t+\angle\gamma(t)+\phi(t)\right)\right). \quad (16)$$

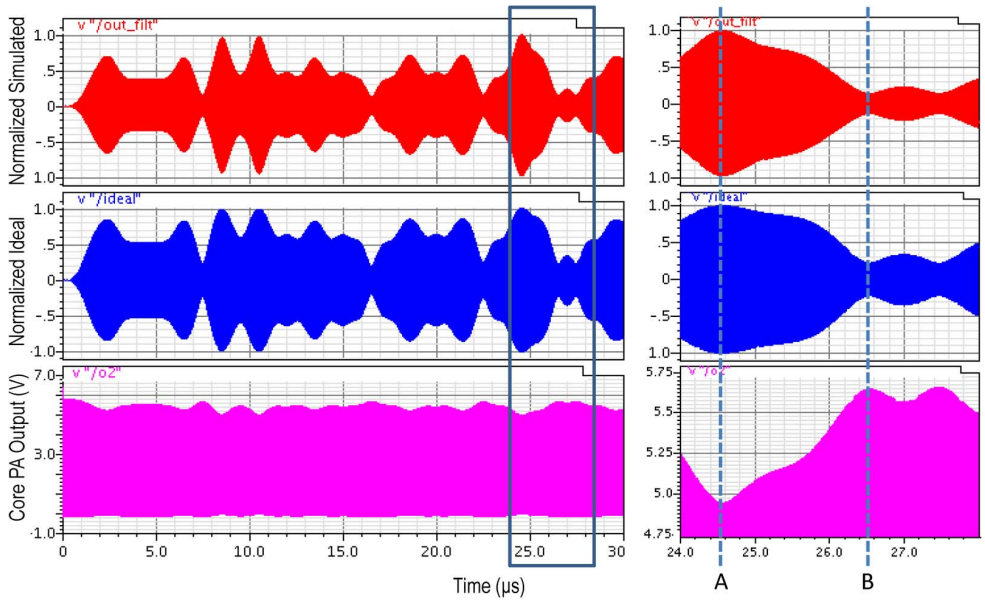

Fig. 8. Simulated output waveform (top), ideal modulation (middle), and core PA output swing (bottom) in Class-B outphasing amplifier with lossless combining. The core PA output swing (shown in the enlarged chart on the right) is not constant. When ϕ is large (point A) the PA is at the edge of compression. For small ϕ (point B) the PA goes into deep compression and the swing becomes larger.

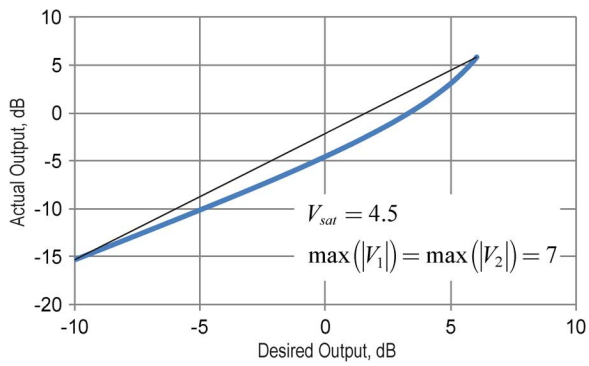

Fig. 9. Clipping distortion in Class-B outphasing amplifier.

Transforming this into the spectral domain,

$$\tilde{X}(f) = X(f) + X_m \mathcal{F}\left[\epsilon \cos\left(\omega_0 t + \angle\gamma(t) + \phi(t)\right)\right] - X_m \mathcal{F}\left[\delta \sin\left(\omega_0 t + \angle\gamma(t) + \phi(t)\right)\right] \quad (17)$$

where the function $\mathcal{F}[\cdot]$ denotes the Fourier transform. The first term in (17) is the undistorted spectrum $X(f)$. Well-conceived modulation schemes [3] will produce a spectral density that decays quickly outside its allocated channel, leaving adjacent channels open for use by others. The second term in (17) is associated with an error spectrum that arises from time-shifted versions of a pure phase modulated (PM) waveform. This spectrum decays gradually over an infinite bandwidth. Depending on the size of the mismatch coefficients ϵ and δ, the gradually decaying spectral density of the error may exceed the residue of the ideal $X(f)$ in adjacent channels. We must find the largest tolerable mismatch before the error spectrum violates specifications on adjacent channel leakage.

The usual approach is to simulate the PM spectrum in each of the two outphasing paths [6]. Using Carson's rule [3], we can estimate the error spectral bandwidth for QAM (see Appendix A). This allows direct calculation of upper bounds on ϵ and δ, which may be quite stringent depending on the adjacent channel leakage that can be tolerated: for example, to meet the mask requirements of a GSM/EDGE transmitter for -60-dBc ACPR the two amplitudes must match to within 0.1 dB (1%). Balancing the two half circuits to this accuracy requires careful layout and, if errors still remain, some form of final calibration. However, if the amplifier is otherwise distortion-free by construction, a one-time calibration should be sufficient to balance the two paths.

IV. Constructing the Outphasing Amplifier

The original circuit of Fig. 2 comprising two outphased voltage sources that drive the terminals of a resistor load is without shortcomings that arise when RF PAs are close to current sources (Fig. 6). The limiter in that figure is a reminder that compression sets in when the apparent load increases and causes the voltage swing to rise. To eliminate this compression, the circuit must be modified to generate constant amplitude sinusoids at each terminal of the load for all outphasing angles.

To make a current source masquerade a voltage source, we could use voltage-sensing feedback that regulates the controlled current source to hold the output voltage to a desired value. Feedback applied around RF circuits, though, runs into problems of stability. The other method is predictive, and this is what we use. When the load is known or changes predictably, then the current source circuit can be regulated, open-loop, to produce a constant load voltage.

Since the outphasing waveforms are, by definition, periodic at the carrier frequency, and of constant amplitude V_A but variable phase, the power amplifier must be adjusted in two different ways to regulate the output voltage in response to the changing load admittance $Y(\phi) = G(\phi) + jB(\phi)$ (see Section III-A).

1) In response to a changing load conductance $G(\phi)$, the *transconductance must change* to maintain *constant*

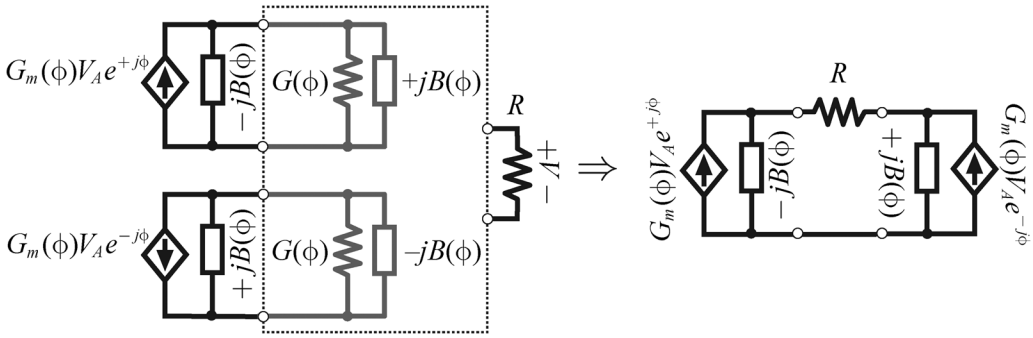

Fig. 10. Class-B outphasing equivalent circuit. Signal-dependent elements substitute voltage sources in Fig. 2.

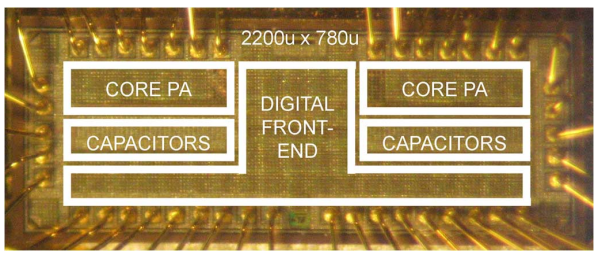

Fig. 11. Chip micrograph.

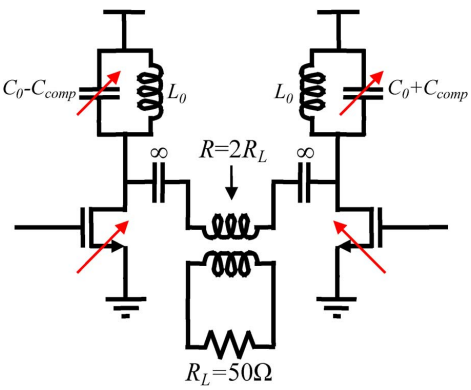

Fig. 12. Outphasing PA with admittance compensation.

voltage amplitude $(G_m(\phi)/G(\phi))V_A$. When the load conductance is small and dissipates little signal power, the transconductance also shrinks, drawing lower bias and signal power from the supply voltage.

2) In response to a changing load susceptance $B(\phi)$, a *variable susceptance* across the transconductor's terminals changes by an equal amount but with opposite sign. This maintains a constant power factor close to 1 and efficiency close to peak (see Section III-A).

Fig. 10 shows the equivalent circuit of an amplifier with these properties. The phasor voltage at the terminals is proportional to $V_A e^{\pm j\phi}$. It follows from the *substitution theorem* of basic circuit theory [21] that when each half-circuit made up of a variable transconductance and susceptance is replaced by an ideal voltage source carrying the terminal voltage waveform, the load cannot tell the difference. The variable transconductance and susceptance are nonlinear elements in the sense that their instantaneous magnitude depends on a signal, the outphasing angle. This arrangement is an instance of an internally nonlinear circuit that appears externally as linear.[7]

V. Outphasing Amplifier Prototype

We have realized a prototype circuit in 90 nm CMOS with the properties described above (Fig. 11) to reconstruct GMSK, EDGE, and WCDMA. This implementation shows feasibility of the concepts developed in this paper at output levels up to about +20 dBm peak [22].

A. Circuit Description

A slightly overdriven Class-B PA provides a high efficiency with moderate insensitivity to small load variations. In this prototype, two such PAs, each with a stand-alone sinewave drain efficiency of 57%, are used with an off-chip lossless combiner. The variable admittance seen by the PAs requires an adaptive circuit, controlled by DSP, to correct the signal-dependent impedances. To cancel the variable susceptance we should add or subtract a shunt reactive element at each PA output. Ideally, this would be a shunt capacitor attached to one side and a shunt inductor to the other, but for practical reasons we add some capacitance to a fixed capacitance on one side and subtract it form the other (Fig. 12). The value of this capacitance $C_{\rm comp}$ as found by noting that its admittance should cancel the susceptance in (5) and (6):

$$C_{\rm comp}(\phi) = \frac{\sin 2\phi}{\omega_0 R}. \tag{18}$$

This *compensating capacitance* depends only on the carrier frequency, the outphasing angle, and value of the load resistance seen across the combiner input ports. After the susceptance is compensated, the remaining apparent resistance, which is the reciprocal of the conductance term in (5) and (6), is a function of the outphasing angle

$$R_{\rm app}(\phi) = \frac{R}{2\sin^2\phi}. \tag{19}$$

To keep the signal swing constant at the output of the PAs, i.e. to counteract dependency to ϕ, the transconductance of the core transistors is scaled by $\sin^2\phi$ to keep the device at the same overdrive level. This eliminates clipping distortion and also saves power at high outphasing angles.

The outphasing inputs applied to the Class-B PAs are in form of two RF square waves at CMOS logic levels. If the square

[7]The transistor current mirror is the most common example of this.

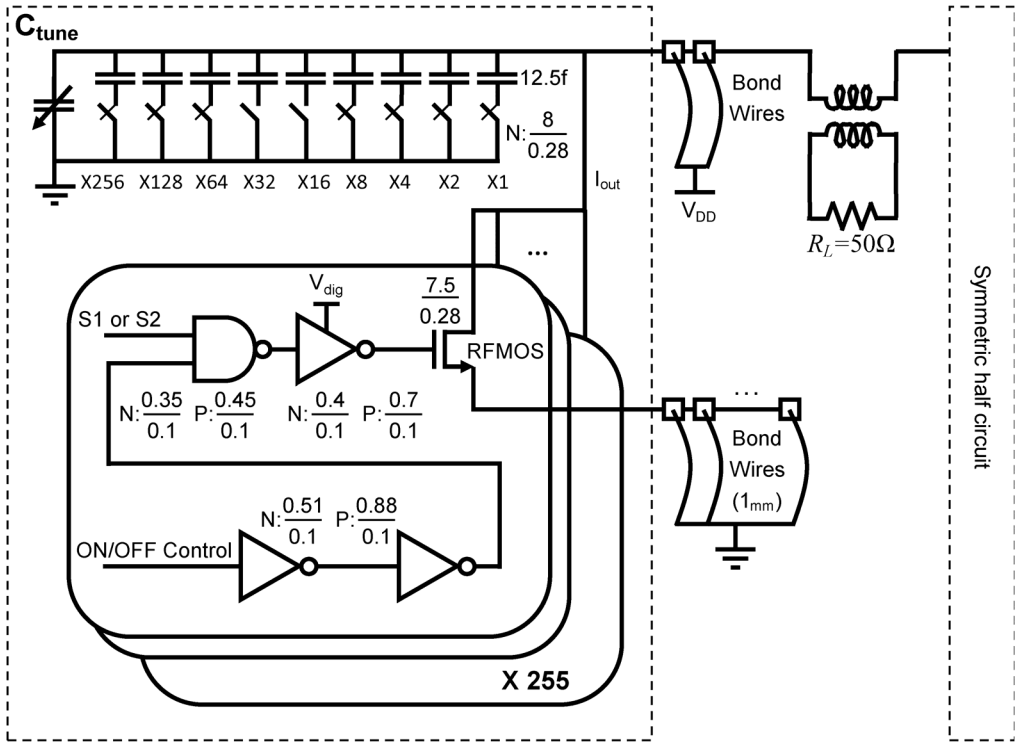

Fig. 13. Circuit diagram of prototype that realizes Fig. 10.

wave is perfect, the drain efficiency will be about 64%. However, if the transition edges of the square-wave are slowed down, the efficiency can be improved up to a maximum of 88%. This also helps to avoid switching spurs in the spectrum. To drive the PAs, we use an all-digital outphasing modulator [23] that synthesizes the two outphasing waveforms $S1$ and $S2$.

The core transistor in each PA is made up of 255 units in parallel, each unit comprising a small FET with 280-nm channel length chosen to withstand the relatively large output voltage swing (Fig. 13). The drains of all FETs are tied together to sum their currents. The outphasing voltage is applied to the gates of all FETs, but only those enabled by the control logic will respond. Thus, the output current can be swept under digital control from 0 to 255 times a small unit outphasing current to make a digitally variable transconductance. The gates can easily toggle at up to 6 GHz in our 90-nm technology. The duty cycle of the driving signal can change its operation from Class C to A/B, which adds another degree of programmability to this prototype. The bias voltage on $S1$ and $S2$ sets this duty cycle. The digital supply $V_{\rm dig}$, nominally at 1.2 V, sets the drive amplitude.

What is shown in Fig. 13 is only half of the complete circuit. A floating resistor load appears in series with the two halves (at the primary terminals of an ideally lossless transformer balun). Each half is driven by one of the outphasing square waves. Attached from the output terminal to ground is an array of switched capacitors, also binary weighted for susceptance control. The output port is tuned to a high impedance at the carrier frequency by resonance between the bondwire inductance and the switchable banks of capacitors. For the reactive compensation a fine 8-bit binary weighted array of 12.5-fF capacitors is used in each PA's tuning tank and set to mid-scale. Then, to maintain a constant power factor with the changing susceptance in the apparent load across each half circuit, the fine capacitance is raised on one side and lowered on the other. In addition, a 6-b array of larger capacitors $C_{\rm tune}$ tunes the load to the desired band of operation. Transistors and capacitors are controlled by a thermometer code and are laid out as 255 intermeshed cells for good matching and monotonic switching.

This is a digital compensation based on the repeated switching of many small PA units and capacitors. Therefore, the resulting spectrum contains quantization noise that becomes smaller as the number of bits in the switchable banks increases. The spectral density of this noise can be simulated. We found the circuit meets the mask requirements for EDGE, WCDMA, and GSM at a reasonable margin with least 8 b for the compensation capacitors and 8 b for the transistor array. Fig. 14 shows the result of the transistor-level simulation and comparison with the ideal modulation for EDGE. In a practical implementation, the quantization noise is not the dominant factor. What limits the noise floor is the phase and amplitude mismatch of the two paths, which we address in Section III-D.

Bondwires are used as inductors at the FET drains. We found that these bondwires, the parasitic capacitance, and the trace inductance on the PCB limited the tuning range of the amplifier's resonance load in this prototype PA to below 1.4 GHz. With more advanced packaging technologies such as flip-chip, which shrinks the parasitics significantly, the circuit can operate at 3 to 6 GHz. The layout of the capacitors was optimized for high Q. Switching of capacitors and transistors with a thermometer code suppresses large glitches arising from differential nonlinearity (Fig. 15) and minimizes the capacitance switching in or out of the tank at each update, thus lowering the disturbance due to charge redistribution after each switching.

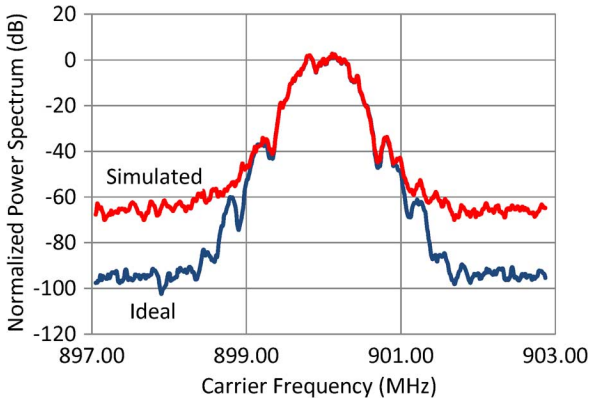

Fig. 14. Ideal modulation and transistor-level simulated outphasing PA output for EDGE modulation (with a symbol rate of 1 Ms/s and 8-b control words).

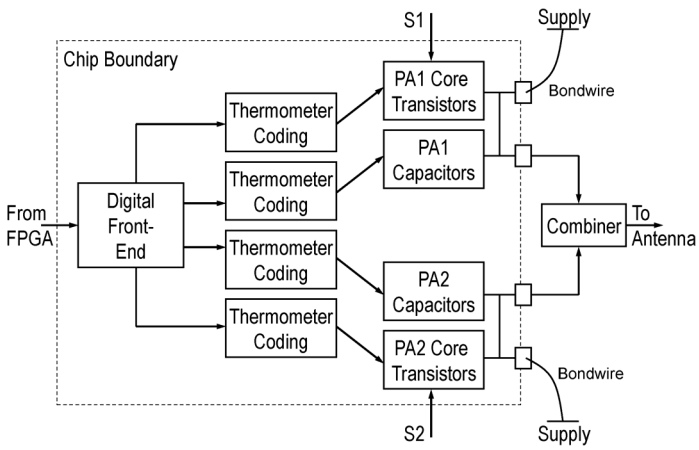

Fig. 15. Thermometer-coded drive of switched elements.

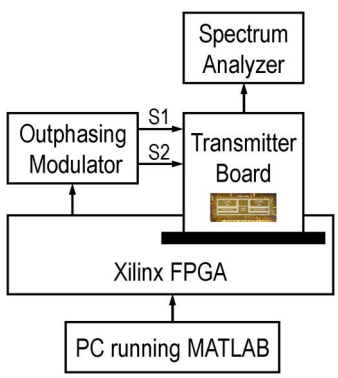

Fig. 16. Test setup.

The test setup for the chip is shown in Fig. 16. A PC precalculates the switching scheme and sends the results to an FPGA which generates data at 68 MHz for different circuit blocks. A high-speed on-chip digital front-end generates the control words that switch FETs and capacitors. A careful timing analysis was necessary to guarantee that the switching of the transistors is synchronized to the capacitors. The edges of the capacitor switching commands are intentionally slowed down to lower the leakage of the 68-MHz clock to the output. Separate grounds were used for digital and RF circuits.

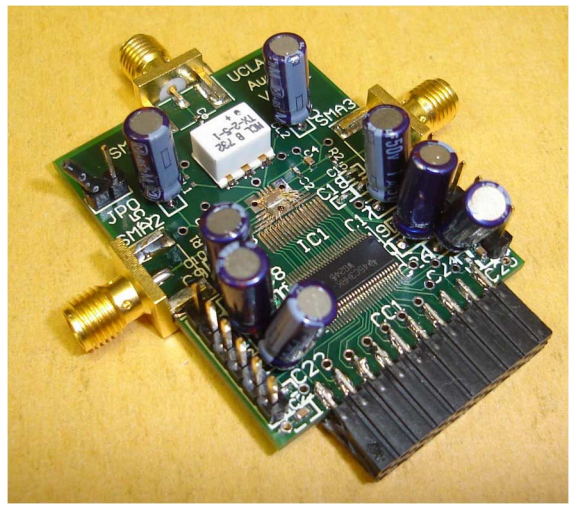

Fig. 17. Transmitter board.

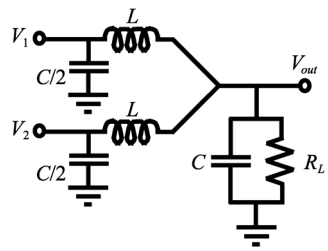

Fig. 18. Lossless combining with an LC network.

The compact transmitter test board is shown in Fig. 17. The outphasing signals are combined in an off-chip (ideally) lossless combiner. There are two choices of combiner. An RF transformer (balun) can provide wideband combining at the price of about 1-dB insertion loss arising from resistance of its windings. An LC combiner (Fig. 18) is almost lossless but it is narrowband around $\omega_0 = 1/\sqrt{LC/2}$. Since the LC combiner in effect adds the two outphasing signals, one of the outphasing signals is inverted in baseband. We used both methods to find the maximum efficiency that can be obtained.

We did not implement an explicit means of power control in this prototype, but within the scope of the outphasing amplifier there are certain options. One possibility that we successfully verified in simulations is to use a subrange of the unit cell array to capture the modulated waveform as power is lowered. For this to provide accurate results the number of bits controlling the switching arrays must increase by one for every 6 dB of gain control. However, only a bit or two may be sufficient for this purpose because at lower power levels the peak amplitude is scaled down, which means the core PAs can operate away from compression. Therefore they revert to normal Class-B mode without compensation, where they can reconstruct the signal in the outphasing form specified by (13).

B. Switch-Induced Distortion

Loss in the nonzero resistance of the FET switches in series with the unit capacitors (Fig. 19) accounts for a small erosion in efficiency, but less obviously the resistance can also be a source of distortion. To simplify the analysis that shows this, we transform the series $R - C$ circuit branches into shunt

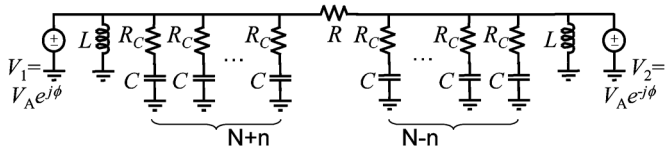

Fig. 19. Switch-induced distortion.

$G-C$ branches. If the switch resistance (R_C) is small compared with the capacitor's reactance at the carrier frequency, i.e., $R_C \ll 1/(\omega_0 C)$, then it is easily seen that the series $(R+jX)$ branch is equivalent at its terminals to a shunt $(G+jB)$ branch through the relation

$$Y(j\omega_0) = \frac{1}{Z(j\omega_0)} \simeq \underbrace{(\omega_0 C)^2 R_C}_{G} + j\underbrace{\omega_0 C}_{B}. \tag{20}$$

Now the capacitor array in our prototype appears as $(N+n(\phi))C$ across one half circuit, and $(N-n(\phi))C$ across the other, where the fixed component NC in parallel with the fixed output inductance is designed to resonate at ω_0, while the variable component $\pm n(\phi)C$ compensates the apparent susceptance across the half-circuit terminals

$$n\omega_0 C = \frac{\sin 2\phi}{R} \quad \Rightarrow \quad n = \frac{\sin 2\phi}{\omega_0 C R}. \tag{21}$$

From (20), we see that, for n unit capacitors turned on by series FET switches, the effective shunt conductance will be nG_C. This will add, or subtract, from the apparent conductance across each half circuit due to the load resistor R, to give a net apparent conductance $\tilde{G}(\phi)$ of

$$\begin{aligned}\tilde{G}(\phi) &= G(\phi) \pm nG_C \\ &= \frac{2\sin^2\phi}{R} \pm n(\omega_0 C)^2 R_C \\ &= \frac{2\sin^2\phi}{R} \pm \frac{R_C}{R}\omega_0 C \sin 2\phi \qquad (22) \\ &= \frac{2}{R}\sqrt{1+(\omega_0 C R_C)^2}\,\sin\phi \sin(\phi \pm \arctan \omega_0 C R_C). \qquad (23)\end{aligned}$$

The second sin term in the product leads to encoding distortion that, although small because $R_C \ll 1/(\omega_0 C)$, cannot be undone by a simple fixed rotation of the encoding angle. The recourse is to remove the undesired dependence of G on ϕ with a compensating resistance. This compensation is effected by a parallel array of switched resistors whose conductance $G_{\text{comp}} \geq 0$ changes inversely with ϕ as follows:

$$G_{\text{comp}} = \frac{R_C}{R}\omega_0 C(1 \mp \sin 2\phi). \tag{24}$$

Due to the high quality factor of the switched capacitors in this prototype $(Q = 40)$, simulations did not indicate noticeably better signal quality after this compensation, and therefore we decided not to include the scheme. For low-Q capacitors, however, the compensation will become necessary. This analysis illustrates an outphasing tradeoff where to remove a small distortion, we must pay the price of a small loss in efficiency due to the additional power lost in G_{comp}.

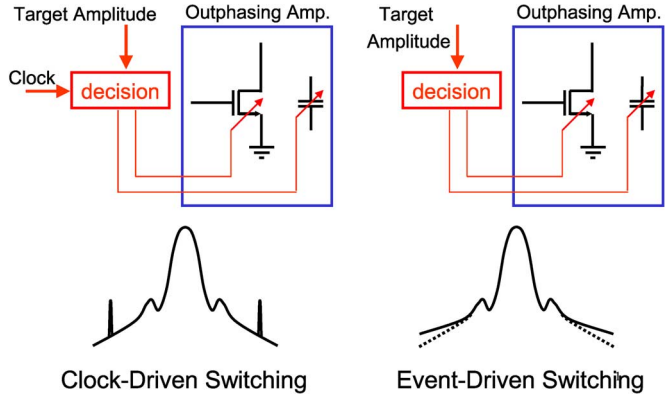

Fig. 20. Output spectra of synchronous switching compared with level-dependent asynchronous switching.

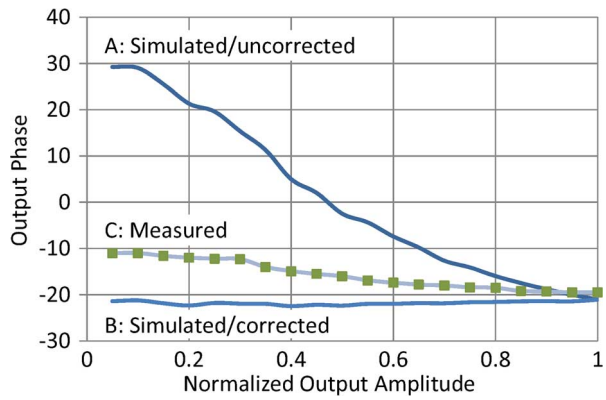

Fig. 21. AM–PM distortion in outphasing amplifier.

VI. Experimental Results and Discussion

A. Accuracy of Waveform Reconstruction

FETs and capacitors in this circuit are clock-driven. The periodic switching may create unwanted tones and spurs in the reconstructed spectrum at the clock frequency and its multiples. We measured acceptably small levels for those spurs at -60 dBc or better, which do not violate the standards that we have investigated. This may not be true for other standards with more demanding spectral purity levels. By randomizing the switching, the energy concentrated in these spectral tones may be dispersed over a wide band. Therefore, when the out-of-band emission is a problem, we can change from clock-driven switching to level-driven switching of elements. In the latter case, capacitors and FETs are switched only when the target amplitude of $x(t)$ crosses certain preset values that resemble thresholds in an A/D converter. The random distribution of amplitudes in a data-bearing modulation will spread the energy of switching over a wide band (Fig. 20).

The outphasing amplifier in our prototype suffers from a deterministic AM-PM distortion. This arises because the effective capacitance at the drain of each unit FET changes when the transistor switches from off to on and vice versa. Therefore, if the resonant tank is tuned to ω_0, say, for $\phi = 90°$ (maximum amplitude), then as the outphasing angle moves towards zero a smaller number of transconductor FET cells are turned on and the resonance shifts away from ω_0. This amplitude-dependent phase shift at the output is AM–PM distortion.

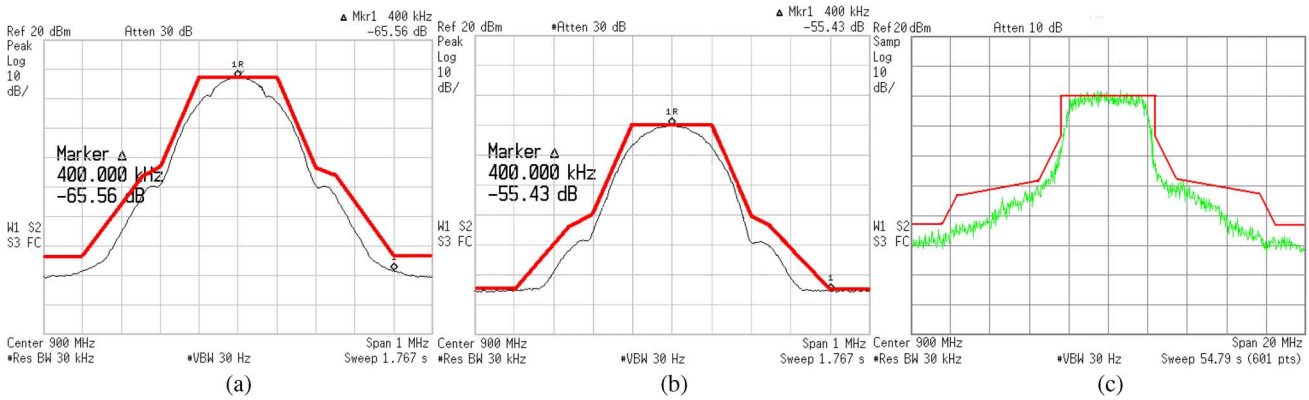

Fig. 22. Measured output spectra. (a) GSM. (b) EDGE. (c) WCDMA.

This effect is apparent in schematic simulations (plot A in Fig. 21) where an excess phase shift as large as 50° is observed across the range of output amplitudes. However, if in the same simulation a small capacitance of 28 fF is switched into the tank for every transconductor that gets switched out the AM-PM conversion can be almost completely removed (Fig. 21, plot B). We decided not to include this auxiliary set of capacitors in hardware. Rather, we incorporated this as an offset into the formula used in the baseband to calculate $C_{\rm comp}$. When the modified formula was used during the measurement, the measured AM-PM conversion was reduced to around 8° (Fig. 21, plot C).

Fig. 22 shows measured spectra of GSM, EDGE, and WCDMA modulations, all at 900 MHz. Table I summarizes the measured EVM. Output power levels are in the range of +13 to +16 dBm, with the output stage supplied at 2.5 V. All spectra lie within the masks set by the standards. Good matching between simulated and measured spectra is clearly seen, for example, by comparing Figs. 14 and 22 (in case of EDGE modulation). A one-time fine adjust is needed to balance the amplitudes at the two half circuits and remove residual AM–PM distortion. Consistent with the analysis in Section III-D, owing to a carefully planned symmetrical signal distribution on-chip, the delays between the signal paths need no adjustment.

TABLE I
MEASURED PHASE ERROR AND SPECIFICATIONS

Standard	Phase Error EVM (rms/max)	Specifications
GSM	2.8° / 11°	5° / 20°
EDGE	4.8% / 13%	9% / 30%
WCDMA	14.8% max	17.5% max

TABLE II
POWER, EFFICIENCY, AND CURRENT CONSUMPTION

Standard	P_{out} (dBm)	η balun	η LC
GSM	16.4	49%	56%
EDGE	13.6	39%	44%
WCDMA	13.0	27%	30%

B. Efficiency

The PA output voltage reconstructed after combining was measured across the 50-Ω input of a spectrum analyzer. Table II lists the power consumption and efficiency for two different configurations. In one, the chip's two output terminals connect through a lossless LC combiner to the load. In the other, they connect through an external RF transformer with impedance transformation ratio of 2 (100 Ω differentially across the chip output). When producing GSM modulation, the lossless combining leads to a drain efficiency very close to the maximum 57% (stand-alone efficiency of the core PAs) because the modulation is with constant envelope. When a balun is used, its 1 dB insertion loss accounts for the lower 49% efficiency.

Measured efficiency for the variable-amplitude modulations, on the other hand, is not as high, even after accounting for the balun loss. For WCDMA modulation the measured average efficiency is only 27%, considerably lower than reasonable values of η_0,[8] the baseline efficiency of this Class B. To understand why this is so, we recognize that across the drain and source of the FET current sources there is a nonzero conductance $G_{\rm loss}$ modeling the loss in the tuning circuit and the transformer at the output. The power dissipated in the apparent load $G(\phi)$ is the useful component because it flows to the intended destination, while power dissipated in $G_{\rm loss}$ is wasted. The apparent load's susceptance has been tuned out by parallel resonance with the switched capacitor array. As the outphasing angle decreases, the efficiency η will also decrease because $G_{\rm loss}$ absorbs an increasing fraction of the power delivered by the amplifier. Expressed in terms of the normalized output amplitude $a = \sin\phi$, the efficiency is

$$\eta(a) = \eta_0 \frac{a^2}{a^2 + \frac{1}{2}RG_{\rm loss}} \tag{25}$$

where R is the resistance across the combiner input ports.

We have measured the sinewave efficiency of the prototype circuit by sweeping a from 0 to 1 (Fig. 23). The data suggest that this amplifier can reach an $\eta_{\max} \simeq 56\%$ at peak amplitude. In our outphasing system $\mathrm{R} = 100\ \Omega$ and based on a quality factor of about 40 for capacitors (10 pF) and bond wire inductors

[8] η_0 is the efficiency of the PA if all losses of the passive elements could be nulled. It is close but below the theoretical maximum because the transistor has internal losses.

TABLE III
COMPARISON WITH OTHER OUTPHASING PAS

Outphasing PA	This work	[17]	[24]	[12]
Fabrication Technology	90 nm CMOS	0.25 μm pHEMT	LDMOS	32 nm CMOS
Area	1.72 mm^2	N/A	N/A	1.28 mm^2
Core PA Operation Mode	Class B	Class B	Class B	Class D
Peak Efficiency	56%	75%	75%	35%
Average Efficiency (WCDMA)	30%	45%	30%	21.8%
ACPR Limit	-50 dBc	-36 dBc	-45 dBc	-40 dBc

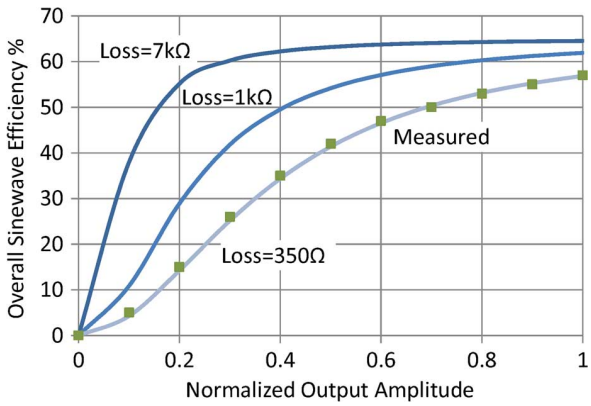

Fig. 23. Sinewave efficiency: measured, calculated, and predicted.

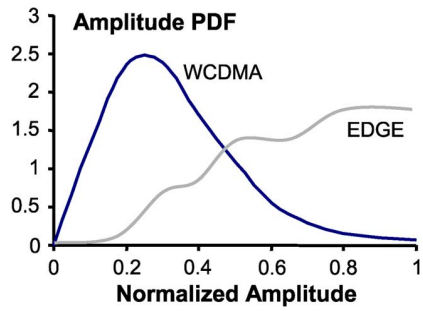

Fig. 24. PDFs of amplitude for EDGE and WCDMA carrying random data.

(3 nH), and other trace losses we estimated $G_{\rm loss} = 1/(350\ \Omega)$ at 900 MHz. With a baseline efficiency of $\eta_0 = 65\%$, the measurement fits the prediction in (25) remarkably well (Fig. 23). This means that a single, constant source of dissipation $G_{\rm loss}$ across the Class-B FET in each half circuit can model the fall in efficiency as the output amplitude drops below the peak value.

Knowing the amplitude probability density function (PDF) $p(a_{\rm WCDMA})$ of a complicated waveform such as WCDMA, the plot of sinewave efficiency may be used to predict the average efficiency. Since the RF waveform is slowly modulated in amplitude,[9] it follows by definition of the average that for a WCDMA waveform

$$\langle \eta \rangle = \int_0^1 \eta(a) p(a_{\rm WCDMA}) da. \tag{26}$$

Fig. 24 shows the characteristic PDF of EDGE and WCDMA. Using this and the measured sinewave data in Fig. 23 to numerically evaluate the integral in (26) gives an average efficiency of 26.7% for WCDMA, in close agreement with the measurements.

VII. CONCLUSION

We have presented a theoretically comprehensive treatment of outphasing systems that use RF high-efficiency Class-B PAs. Our analysis shows that the nonlinearity and distortion commonly reported in the outphasing literature can be explained and accounted for by applying the principles of basic circuit theory.

[9]"Slowly modulated" means that many hundreds or thousands of cycles of the RF carrier frequency will elapse before the WCDMA modulation changes its amplitude measurably. The power amplifier responds quasi-statically over this time scale by delivering many cycles of the carrier frequency at a nearly constant amplitude at the associated efficiency.

We have isolated forms of distortion that are unique to outphasing, and the insights gained from that analysis have led us to criteria for highly efficient and distortion-free outphasing PAs. We have realized these techniques in a 90-nm Class-B prototype that uses signal-dependent time-varying circuits under intimate digital control with lossless combiners to achieve 56%, 44%, and 30% efficiency, for GSM, EDGE, and WCDMA modulations, meeting the mask and linearity requirements and accomplishing ACPR of up to -50 dBc. Using distortion for WCDMA modulation as a figure of merit, Table III shows that this realization demonstrates a very good outphasing ACPR, where the only calibration involved is the gain balancing and a fixed predetermined AM/PM correction. Problems arising from package parasitics or the ON resistance of compensation switches have been identified and solutions to them proposed.

APPENDIX A
PM BANDWIDTH OF QAM

Carson's rule states [3] that the effective (-40 dB) bandwidth B of the pure PM waveform $\cos(m(t))$ is

$$B \approx 2 \times (\max |m(t)| + 1) \times W \tag{27}$$

where the information waveform $m(t)$ itself occupies the bandwidth W and is of mean value zero. Consider M-ary QAM occupying 1-Hz bandwidth synthesized by an outphasing modulator. This means that, every second, the phase θ jumps by some amount uniformly distributed in the interval $(-\pi, +\pi)$. The QAM waveform amplitude also jumps by some other amount that is uniformly distributed in the interval $(-V_p, +V_p)$, where V_p is the peak of the QAM envelope. Since the outphasing angle ϕ determines amplitude, it must be distributed *non*-uniformly (because $V \propto \sin\phi$) in the interval $(0, +\pi/2)$. Since Carson's rule as stated applies to a zero-centered waveform, we shift this interval to $(-\pi/4, +\pi/4)$. Then to make the analysis simple, we assume that the outphasing

angle is distributed uniformly in this interval. Now, applying (27), the effective bandwidth B of the phase-modulated waveform $\cos(\pm\phi(t) + \theta(t))$ that will be present in each of the two outphasing paths is

$$B \approx 2 \times \left(\pi + \frac{\pi}{4} + 1\right) \times 1 = \frac{9\pi}{2} \simeq 13. \qquad (28)$$

This expression does not depend on M, which is the number of points in the QAM constellation, so whatever M the spectral density of the outphasing waveform stretches across 6.5 channel widths on each side of its own carrier until it has decayed by 40 dB relative to its peak. Equation (28) predicts that the power spectral density for both 16-QAM and QPSK (4-QAM) modulations drops by about 35 dB and levels off at a distance of 6 channel widths from the carrier. [6, p. 66] shows simulated spectra of outphasing waveforms for four different modulations, which agrees with these findings.

ACKNOWLEDGMENT

The authors would like to thank K. Takinami, M. Youssef, M. Mikhemar, E. Heidari, and M. Lee. They are grateful to ST-Microelectronics for chip fabrication.

REFERENCES

[1] R. D. Thornton, J. G. Linvill, E. R. Chenette, H. L. Ablin, J. N. Harris, A. R. Boothroyd, J. Willis, and C. L. Searle, *Handbook of Basic Transistor Circuits and Measurements*, ser. SEEC Series. New York, NY, USA: Wiley, 1966.

[2] H. E. Rowe, *Signals and Noise in Communication Systems*. Princeton, NJ, USA: Van Nostrand, 1965.

[3] S. Haykin and M. Moher, *Introduction to Analog and Digital Communications*. Hoboken, NJ, USA: Wiley, 2007.

[4] H. J. Carlin and A. B. Giordano, *Network Theory*. Englewood Cliffs, NJ: Prentice-Hall, 1964.

[5] D. M. Pozar, *Microwave Engineering*. Hoboken, NJ, USA: Wiley, 2005.

[6] X. Zhang, L. E. Larson, and P. M. Asbeck, *Design of Linear RF Outphasing Power Amplifiers*. Norwood, MA, USA: Artech House, 2003.

[7] P. A. Godoy, D. J. Perreault, and J. L. Dawson, "Outphasing energy recovery amplifier with resistance compression for improved efficiency," *IEEE Trans. Microw. Theory Tech.*, vol. 57, no. 12, pp. 2895–2906, Dec. 2009.

[8] H. Chireix, "High power outphasing modulation," *Proc. Inst. Radio Engineers*, vol. 23, no. 11, pp. 1370–1392, 1935.

[9] F. Raab, "Efficiency of outphasing RF power-amplifier systems," *IEEE Trans. Commun.*, vol. COM-33, no. 10, pp. 1094–1099, Oct. 1985.

[10] S. C. Cripps, *Advanced Techniques in RF Power Amplifier Design*. Norwood, MA, USA: Artech House, 2002.

[11] M. E. Van Valkenburg, *Network Analysis*. Englewood Cliffs, NJ, USA: Prentice-Hall, 1974.

[12] H. Xu, Y. Palaskas, A. Ravi, M. Sajadieh, M. A. El-Tanani, and K. Soumyanath, "A flip-chip-packaged 25.3 dBm class-D outphasing power amplifier in 32 nm CMOS for WLAN application," *IEEE J. of Solid-State Circuits*, vol. 46, no. 7, pp. 1596–1605, 2011.

[13] N. O. Sokal and A. D. Sokal, "Class E-A new class of high-efficiency tuned single-ended switching power amplifiers," *IEEE J. Solid-State Circuits*, vol. SSC-10, no. 3, pp. 168–176, Jun. 1975.

[14] J. Yao and S. I. Long, "Power amplifier selection for LINC applications," *IEEE Trans. Circuits Syst. II, Exp. Briefs*, vol. 53, no. 8, pp. 763–767, Aug. 2006.

[15] F. H. Raab, "Class-E, Class-C, and Class-F power amplifiers based upon a finite number of harmonics," *IEEE Trans. Microw. Theory Tech.*, vol. 49, no. 8, pp. 1462–1468, Aug. 2001.

[16] A. Birafane and A. B. Kouki, "On the linearity and efficiency of outphasing microwave amplifiers," *IEEE Trans. Microw. Theory Tech.*, vol. 52, no. 7, pp. 1702–1708, Jul. 2004.

[17] I. Hakala, D. K. Choi, L. Gharavi, N. Kajakine, J. Koskela, and R. Kaunisto, "A 2.14-GHz Chireix outphasing transmitter," *IEEE Trans. Microw. Theory Tech.*, vol. 53, no. 6, pp. 2129–2138, Jun. 2005.

[18] C. P. Conradi, R. H. Johnston, and J. G. McRory, "Evaluation of a lossless combiner in a LINC transmitter," in *Proc. IEEE Canadian Conf. Electr. Comput. Eng.*, Edmonton, AB, Canada, 1999, vol. 1, pp. 105–110.

[19] S. Hamedi-Hagh and C. A. T. Salama, "CMOS wireless phase-shifted transmitter," *IEEE J. Solid-State Circuits*, vol. 39, no. 8, pp. 1241–1252, Aug. 2004.

[20] C. Rapp, "Effects of HPA-nonlinearity on a 4-DPSK/OFDM-signal for a digital sound broadcasting system," in *Proc. Eur. Conf. Satellite Commun.*, Liege, 1991, vol. 1, pp. 179–184.

[21] C. A. Desoer and E. S. Kuh, *Basic Circuit Theory*. New York, NY, USA: McGraw-Hill, 1969.

[22] S. Moloudi, K. Takinami, M. Youssef, M. Mikhemar, and A. Abidi, "An outphasing power amplifier for a software-defined radio transmitter," in *Proc. Int. Solid-State Circuits Conf.*, San Francisco, CA, USA, 2008, pp. 568–636.

[23] M. E. Heidari, M. Lee, and A. A. Abidi, "All-digital outphasing modulator for a software-defined transmitter," *IEEE J. Solid-State Circuits*, vol. 44, no. 4, pp. 1260–1271, Apr. 2009.

[24] A. Huttunen and R. Kaunisto, "A 20-W Chireix outphasing transmitter for WCDMA base stations," *IEEE Trans. Microw. Theory Tech.*, vol. 55, no. 12, pp. 2709–2718, Dec. 2007.

Shervin Moloudi (M'99) received the B.S. degree in electronics engineering from Sharif University of Technology, Tehran, Iran, in 1995, the M.S. degree in digital signal processing from Tampere University of Technology, Tampere, Finland, in 1998, and the Ph.D. degree in integrated circuits and systems from the University of California, Los Angeles, CA, USA, in 2008.

He was with Nokia Mobile Phones from 1996 to 1998 and Broadcom Corporation from 1998 to 2006. Currently, he is a Principal Manager with Qualcomm-Atheros Inc., Irvine, CA, USA. His primary field of interest is in telecommunication analog and high-frequency circuit design.

Asad A. Abidi (F'96) received the B.Sc. degree (with honors) from Imperial College, London, U.K., in 1976, and the M.S. and Ph.D. degrees in electrical engineering from the University of California, Berkeley, CA, USA, in 1978 and 1981, respectively.

From 1981 to 1984, he was with Bell Laboratories, Murray Hill, NJ, USA, as a Member of the Technical Staff with the Advanced LSI Development Laboratory. Since 1985, he has been with the Electrical Engineering Department, University of California, Los Angeles, CA, USA, where he is Chancellor's Professor. He was a Visiting Faculty Researcher with Hewlett-Packard Laboratories in 1989. His research interests include RF CMOS design, high-speed analog integrated circuit design, and data conversion.

Dr. Abidi is a member of the U.S. National Academy of Engineering and Associate Fellow of TWAS—The Science Academy of the Developing World. From 1992 to 1995, he was Editor for the IEEE JOURNAL OF SOLID-STATE CIRCUITS. He was the recipient of an IEEE Millennium Medal, the 1988 TRW Award for Innovative Teaching, the 1997 IEEE Donald G. Fink Award, the 2007 Lockheed-Martin Award for Excellence in Teaching, and the 2008 IEEE Solid-State Circuit Society's Donald O. Pederson Award. He was named one of the top ten contributors to the ISSCC in its first 50 and 60 years.